

Supplementary Information for

Hybridizing CH₃NH₃PbBr₃ microwire and tapered fiber for efficient light collection

Zhiyuan Gu,^a Wenzhao Sun,^a Kaiyang Wang,^a Nan Zhang,^a Chen Zhang,^b Quan, Lyu,^a Jiankai Li,^a Shumin Xiao^{*b} and Qinghai Song^{*a}

^aNational Key Laboratory on Tunable Laser Technology, Integrated Nanoscience Lab, Department of Electrical and Information Engineering, Harbin Institute of Technology, Shenzhen, 518055, China. E-mail: qinghai.song@hitsz.edu.cn

^bNational Key Laboratory on Tunable Laser Technology, Integrated Nanoscience Lab, Department of Material Science and Engineering, Harbin Institute of Technology, Shenzhen, 518055, China. E-mail: shuminxiao@hitsz.edu.cn

In the main text, we have experimentally investigated the hybrid structure consisted of tapered fiber and CH₃NH₃PbBr₃ microwire. The collected light from the single-mode fiber end is an order of magnitude larger than the collected emission with a 40× objective lens. In this supplemental information, we show the detail information of the simulation model to estimate the collection efficiency by the objective lens. The three-dimensional transmission model has also been described to interpret the coupling mechanism between tapered fiber and perovskite microwire.

1. Synthesis of $\text{CH}_3\text{NH}_3\text{PbBr}_3$ perovskite microwires

We synthesized the $\text{CH}_3\text{NH}_3\text{PbBr}_3$ perovskite microwires by using the one-step solution self-assembly method developed in Ref. S1. First, 0.1 M $\text{CH}_3\text{NH}_3\text{Br}$ and 0.1M PbBr_2 solutions was made by dissolving $\text{CH}_3\text{NH}_3\text{Br}$ (0.105g, 0.1 mmol, Shanghai MaterWin New Materials Cooperation) and PbBr_2 (0.345g, 0.1 mmol, Shanghai MaterWin New Materials Cooperation) in 5ml DMF (N,N-dimethylformamide). Then equal volumes of these two solutions were mixed to obtain a new solution $\text{CH}_3\text{NH}_3\text{Br}\cdot\text{PbBr}_2$ (0.05 M). Next, 15 μL of this new solution was drop-coated onto an ITO glass. Then the ITO glass with coated solution was placed on a Teflon stage in a 250 ml beaker. The beaker was sealed by Parafilm (PM-996) and contained 75 ml CH_2Cl_2 leveled below the Teflon stage. The $\text{CH}_3\text{NH}_3\text{PbBr}_3$ perovskite microwires were finally obtained after evaporation of the new solution for 24 – 30 h.

2. Structural characterization of perovskite microwire

To investigate the structural properties, the X-ray diffraction (XRD) spectrum and energy-dispersive X-ray spectroscopy (EDS) were measured. As the Fig. S1(a) shows, the energy-dispersive X-ray spectroscopy analysis shows the Br/Pb ratio is 72/28, which matches the PbBr_3 stoichiometry well. In addition, the XRD spectrum in Fig. S1(b) indicates the good crystal quality of the sample and the as-synthesized $\text{CH}_3\text{NH}_3\text{PbBr}_3$ perovskite microwires is dominated by (001) series of peaks.

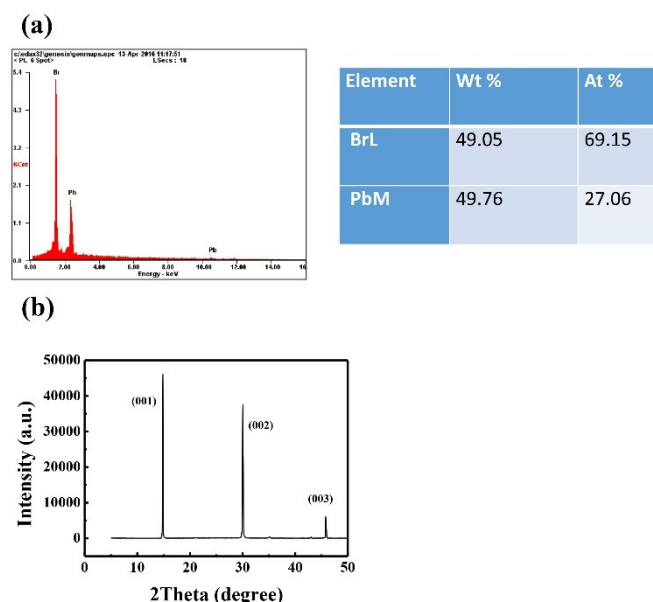


Figure S1 (a) the energy dispersive X-ray spectroscopy (EDS) analysis of the perovskite microwire. (b) the X-ray diffraction (XRD) spectrum of the synthesized perovskite microwire.

3. The measurement of the beam spot size

A microdisk with known size is illuminated by the pump laser. Then a CCD camera was used to take a picture of the sample, as Fig. S2 shows below. The red circle in Fig. S2(a) presents the coverage of the beam spot. Fig. S2(b) is the SEM image of the microdisk. And the measured size of the beam spot is about 58 microns.

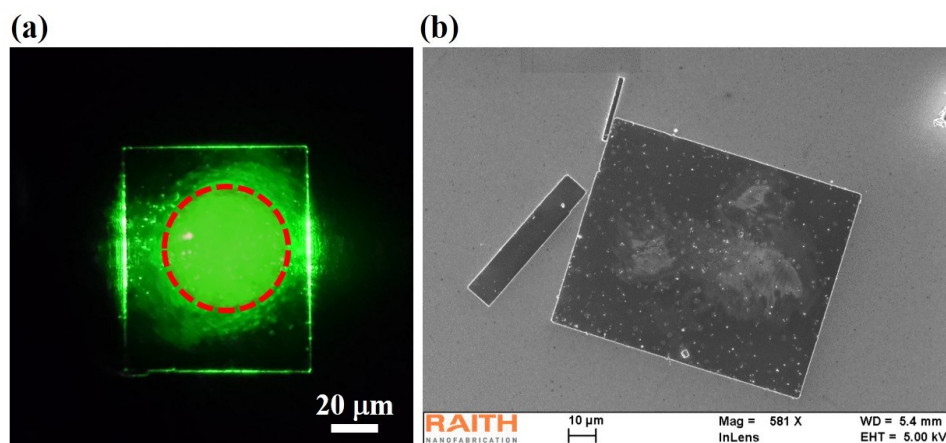


Figure S2 The measurement of the beam spot size. (a) The optical image of the beam spot. (b) the microdisk used to measure the spot size.

4. Laser properties of the hybridizing structure

In Figure 2(c) of the main text, we integrated the intensity of all the laser peaks within the whole wavelength range. The threshold is around $17.5 \mu\text{J}/\text{cm}^2$. To investigate the threshold of each peak contained in the spectrum of Figure 2(b), the intensity of each peak was integrated separately. The result is summarized in Figure S3 below. We can see that all the peaks exhibit the similar laser threshold around $17.5 \mu\text{J}/\text{cm}^2$ and slope of the “S” curve.

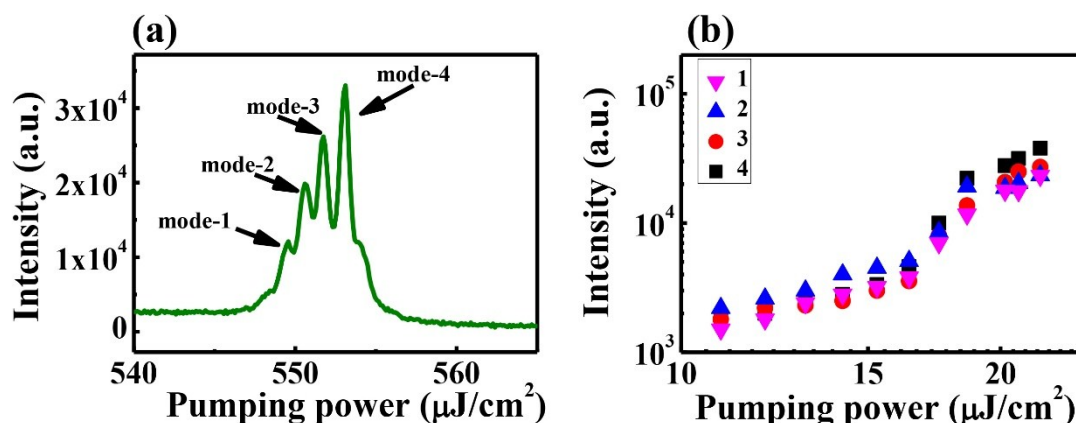


Figure S3 (a) four peaks marked mode-1, mode-2, mode-3 and mode-4 in the laser spectrum are integrated separately to obtain the light-light curve (b).

5. Light collection in hybridizing $\text{CH}_3\text{NH}_3\text{PbBr}_3$ microwire and tapered fiber

To validate the reproducibility of the proposed hybrid structures, additional experiments were performed. As shown in Fig. S4 below, the recorded laser spectra from the end of tapered fiber and from the objective lens are presented. The intensities collected from the tapered fiber are more than an order of magnitude higher than the ones from the high NA objective lens, indicating the efficient light collection of the tapered fiber. The top panels in the Figure are the fluorescent microscope images of the microwire lasers.

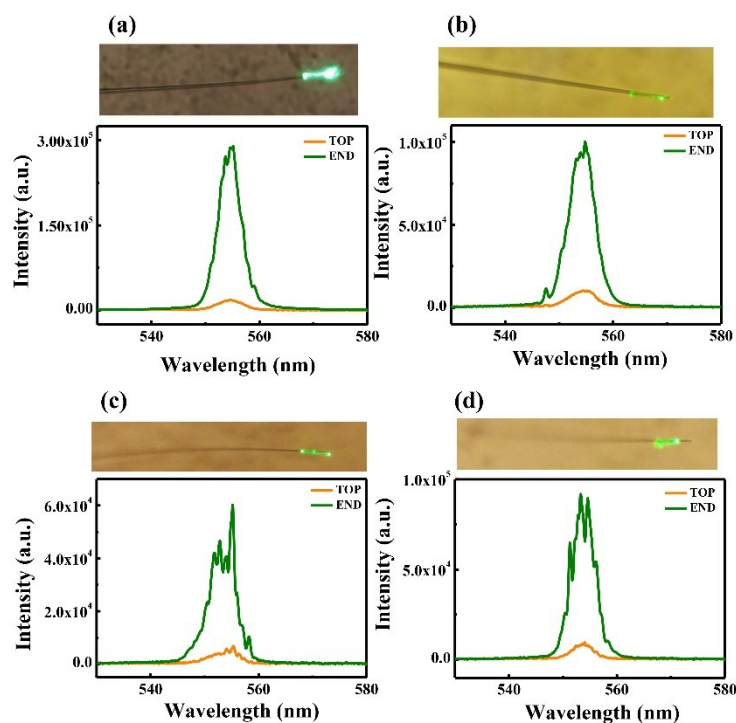


Figure S4 The recorded laser spectra from the end of tapered fiber and from the objective lens and fluorescent microscope images of the microwire lasers.

6. Two-dimensional simulation model of the hybrid structure

For the hybrid structure, the emitted lights were collected by the objective lens. In this situation, the collected lights via objective lens is mainly the scattered light or radiative light. Here, we employ a two-dimensional numerical model to calculate the collection efficiency. The simulation configuration is shown in Figure S5, a perovskite microwire is placed on the silica substrate. The refractive index of $\text{CH}_3\text{NH}_3\text{PbBr}_3$ perovskite microwire and silica fiber are 2.55 and 1.46, respectively. For simplicity, a flat silica substrate is considered. Here we take the size of the microwire as $1.05 \times 1.01 \mu\text{m}^2$, which are the same as the sample used in Figure 2 of main text. A two-dimensional numerical simulation (Finite elements method, Comsol Multiphysics 4.4) has been performed to examine the wave propagation of the microwire. A transverse mode

(H is perpendicular to the microwire axis) is used to excite the microwire. The calculated field pattern is shown in Figure S5. The emitted lights are divided into the following parts, i.e., reflected, transmitted, radiative and leaked lights. By performing the overlap integrals of the simulated field distribution, we can roughly estimate the reflected, transmitted, radiative and leaked energy efficiency. The calculated reflection at the microwire-air interface is about 26 %. About 45.7% of the energy crosses the wire-air boundary and then propagates straight. From the field distribution, we also can find that partial energy leaks to the substrate. The integrated energy is about 13.8%. Consequently, the scattered light to the far-field is about 14.5%. The objective lens only collects part of the scattering light. We note that the percentage of energy leaked into the substrate matches the experimental results well. And the value can be further increased by decreasing the size of microwire.

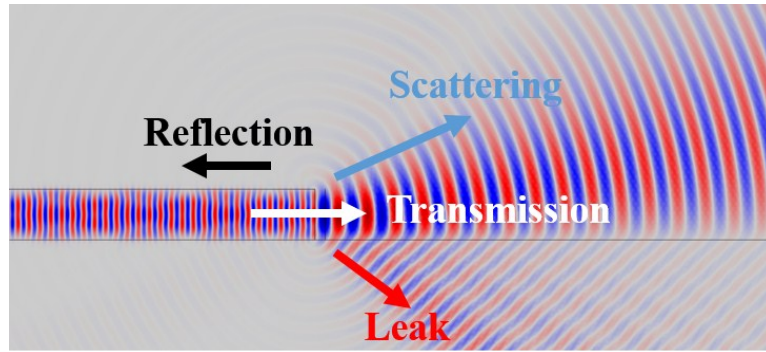


Figure S5 Field distribution of the microwire placed on silica substrate.

7. Extraction efficiency of the microlaser via objective lens

Based on the theoretical analysis in previous section, we can estimate the collection efficiency of objective lens by using the model in Ref. S2. From the field distribution in Figure S5, the scattered light distribution $f(\theta)$ is defined in Figure S6 (red line) [S2, S3]. The green shade represents the total cover angle of the objective lens. It can be seen that the objective lens can only collect part of the scattered light, indicated by the overlap region of green shade and red line. Thus the extraction efficiency can be expressed as

$$\eta_{ext} = \frac{P(\sin^{-1}(0.4))}{P(\pi/2)} \quad (1)$$

In equation (1), $P(\alpha) = 4\pi \int_0^\alpha f(\theta) \sin^2(\theta) d\theta$ is the integrated power at given scattered angle

α . For the objective lens with NA = 0.6, the collection angle α is 36.86 °. Thus the integrated power of overlap region, which is the collected scattered light via objective lens, is about 7%. Since 14.5% of the laser emission is scattered to far-field and only 7% of this can be collected by lens. Thus we can estimate that about 1.07% of the laser emission can be collected by the objective lens.

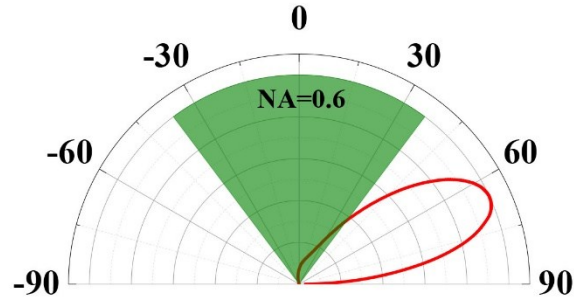


Figure S6 Distribution of the scattered light. The objective lens used in experiment is 40× with NA=0.6. The green shaded region represents the cover angle of the lens. Red line represents the scattered light to far-field of the microwire.

8. Calculation of the coupling efficiency via three-dimensional FDTD transmission model

In the main text, we have also numerically calculated the three-dimensional transmission model (Finite Difference Time Domain, FDTD), which can be used to evaluate the coupling efficiency between tapered fiber and $\text{CH}_3\text{NH}_3\text{PbBr}_3$ microwire. For simplicity, the total length of the tapered fiber is fixed as 100 μm . As shown in Figure S5, the diameter of the tapered fiber at port-2 is fixed as $r_2 = 1.25 \mu\text{m}$. The tilted angle is varied by changing the diameter r_1 of the tapered fiber at port-1. Here, we mainly change two parameters to optimize to coupling efficiency of the hybrid system, the size of microwire, L , and the radius of tapered fiber, r_1 . A transverse mode (TM, H is perpendicular to microwire axis) mode incidents to the structure at port-1. The red arrow indicates the propagation direction. Because the lasing wavelength of the $\text{CH}_3\text{NH}_3\text{PbBr}_3$ microwire is around 550 nm, thus we only consider the transmission efficiency at wavelength 550 nm.

In the three-dimensional transmission model, the coupling efficiency η_{cou} is defined as the

ratio of the power S_2 at port-2 and power S_1 at port-1, $\eta_{cou} = \frac{S_2}{S_1}$.

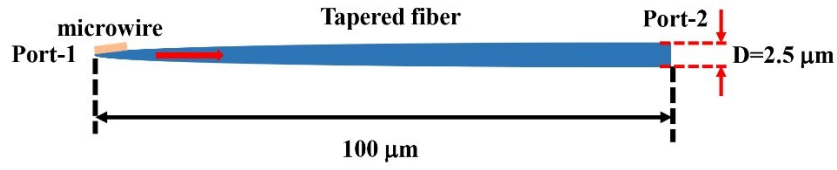


Figure S7 Schematic picture the simulation model. The total length of the tapered fiber is 100 μm . The diameter at port-2 is fixed as 2.5 μm , while changing the diameter at port-1.

9. Three-dimensional transmission of the tapered fiber

To investigate the propagation loss of the tapered fiber, the transmission of the individual tapered fiber without microwire at wavelength 550 nm has been calculated. All the parameters used here are the same as Figure S5. The simulated transmission is plotted as a function of the radius r_1 . The results are summarized in Figure S6. We can see that the transmission is as high as 99.5% with only slight change. Thus the excellent performance of the tapered fiber don't introduce additional loss into the hybrid structure.

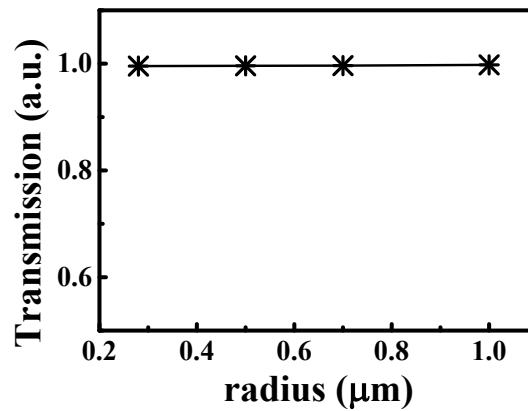


Figure S8 Transmission of the tapered fiber. (a)the schematic picture of the simulated model. (b)the calculated transmission is plotted as a function of the radius of the tapered fiber at port-1. Here we fix the diameter of tapered fiber at port-2 as 2.5 μm .

Reference

[S1] Q. Liao, K. Hu, H. H. Zhang, X. D. Wang, J. N. Yao, & H. B. Fu. Perovskite microdisk microlasers self-assembled solution. *Adv. Mater.* **27**, 3405–3410 (2015).

[S2] R. F. Oulton, V. J. Sorger, T. Zentgraf, R-M. Ma, C. Gladden, L. Dai, G. Bartal, & X.

Zhang. Plasmon lasers at deep subwavelength scale. *Nature*, **461**, 629 (2009).

[S3] Y-H. Chou, B-T. Chou, C-K. Chiang, Y-Y. Lai, C-T, Yang, H. Li, T-R. Lin, C-C. Lin,

H-C. Kuo, S-C. Wang, & T-C. Lu. *ACS Nano*, **9**, 3978 (2015).